THE ASTROPHYSICAL JOURNAL, 440:132–140, 1995 February 10

LOW-LUMINOSITY ACTIVE GALAXIES: ARE THEY SIMILAR TO SEYFERT GALAXIES?

A. KORATKAR,[1] S. E. DEUSTUA,[2] T. HECKMAN,[1] A. V. FILIPPENKO,[3] L. C. HO,[3] AND M. RAO[1]

Received 1994 May 9; accepted 1994 August 26

ABSTRACT

A careful X-ray study of five low-luminosity active galactic nuclei (LLAGNs) was conducted to address specifically the issue of whether the dominant X-ray production mechanism is the same at all luminosities in AGNs. The sample consists of three Seyfert 1 galaxies (NGC 4639, NGC 5033, and NGC 5273), and two low-ionization nuclear emission-line regions (NGC 3642 and NGC 4278) having a weak, broad component of Hα emission.

We find that the X-ray emission (*ROSAT* HRI) is mostly or entirely nuclear ($\lesssim$500 pc) despite the low X-ray luminosities ($\sim 9 \times 10^{40}$ ergs s^{-1}) of the sample. The correlation between X-ray luminosity and the broad Hα emission-line luminosity observed in high-luminosity active galaxies continues down to the low-luminosity range; the mean $L_X/L_{H\alpha}$ ratio of LLAGNs is approximately 14, while that of AGNs is approximately 29. *ROSAT* PSPC observations of three LLAGNs in our sample indicate that the 0.2–2.2 keV X-ray spectral energy distributions are similar to those seen in Seyfert nuclei but do not have high intrinsic absorbing columns. Using existing ultraviolet data for four LLAGNs, we find that the "optical" (2500 Å) to X-ray spectral index (α_{OX}) has an average upper limit of 1.6; for comparison, the measured value in AGNs is typically 1.4, while that in M81 (the prototypical LLAGN) is 1.0.

Subject headings: galaxies: active — galaxies: nuclei — galaxies: Seyfert — X-rays: galaxies

1. INTRODUCTION

Over the past two decades, it has been well established that there is activity in the nuclei of galaxies over a wide range of luminosities. Observations of activity in the nuclei of galaxies from the most energetic (quasars) to the mildly energetic (Seyfert galaxies, and some low-ionization nuclear emission-line regions [LINERs; Heckman 1980]) show that many of the properties are similar and the objects might be related to each other. From the correlation of the optical continuum luminosity with the Hβ luminosity (Yee 1980; Shuder 1981), it has been demonstrated that the bright active galactic nuclei (AGNs) are related and form a luminosity sequence ranging from the highest luminosity quasars down to the more moderate luminosities found in Seyfert nuclei. The discovery of an active nucleus in M81 (Peimbert & Torres-Peimbert 1981; Filippenko & Sargent 1988) pushed the lower limit on the luminosity of an active nucleus to $M_B = -13$ mag, and in NGC 4395 (Filippenko & Sargent 1989; Filippenko, Ho, & Sargent 1993) to $M_B = -10$ mag, comparable to the luminosity of the brightest known stars. In view of this evidence for a luminosity sequence, it is natural to ask if low-level activity in otherwise "normal" galaxies (Heckman 1980; Rose & Searle 1982; Stauffer 1982a, b; Keel 1983a, b; Phillips, Charles, & Baldwin 1983; Rose & Cecil 1983; Filippenko & Sargent 1985, 1986; Phillips et al. 1986) is in any way related to the more luminous classical AGNs. Further, it is crucial to determine whether the basic mechanism that powers the activity is the same in all galaxies and whether the properties of the activity just scale with nuclear luminosity.

LINERs are very common in the local universe according to the optical surveys mentioned above. If the mechanism that energizes LINERs is similar to that of the more luminous AGNs, then the former will have important implications for the faint end of the AGN luminosity function (which is currently very poorly constrained for $L_X \approx 10^{41}$ ergs s^{-1} in the 0.2–10 keV band) and for AGN evolution. LINERs are also detected in the X-rays and may contribute significantly to the cosmic soft X-ray background. Recent results indicate that AGNs can contribute from 30% to 90% of the background at 2 keV (Boyle et al. 1993), but the most luminous quasars account for only 30% of the background (Boyle, Jones, & Shanks 1991). Could low-luminosity active galactic nuclei (LLAGNs) make up the rest of the X-ray background?

The continuity of properties from the most luminous objects to the lowest luminosity AGNs in nearby galaxies is an attractive idea, yet this continuity has not yet been established from moderate to very low luminosities. It is possible that there might be a lower limit to the activity (like the mass limit in main-sequence stars) below which a fundamentally different mechanism is required to power the nucleus. Hence, it is important to determine whether all low-luminosity nuclei exhibiting activity, or a certain subset of them, are genuinely related to classical AGNs, or whether instead their properties might be due to other physical processes.

At the lowest nuclear luminosities several alternative sources of energy responsible for powering the emission-line gas have been proposed. These are reviewed in detail by Heckman (1987), Terlevich, Melnick, & Moles (1987), Filippenko (1989), and Terlevich et al. (1992). Suggestions include (1) photoionization by a dilute version of the nonstellar energy source found in Seyfert nuclei, (2) ionization by starburst driven winds, (3) radiative cooling of accretion flows from galaxy halos, (4) shock heating by compact supernovae in high-density environments, and (5) photoionization by unusually hot O type stars. There is much evidence suggesting that all of the above mechanisms could contribute to the observed nuclear line emission in some

[1] Space Telescope Science Institute, 3700 San Martin Drive, Baltimore, MD 21218.
[2] Institute of Geophysics and Planetary Physics, Lawrence Livermore National Laboratory, 7000 East Avenue, Livermore, CA 94550.
[3] Department of Astronomy, University of California, Berkeley, CA 94720-3411.

galaxies, indicating that LLAGNs are a heterogeneous class of objects (Heckman 1987; Filippenko 1994).

The presence of a broad ($\gtrsim$1000 km s^{-1}) Hα emission-line component, a nonstellar continuum, and emission lines spanning a wide range of ionization states has been interpreted as evidence for low-luminosity nonstellar, quasarlike activity (e.g., Halpern & Steiner 1983; Filippenko & Sargent 1985). Furthermore, detailed spectroscopic studies of individual objects have suggested that the physical processes providing the energy in at least some LLAGNs are similar to those found in their more luminous counterparts (e.g., Filippenko & Halpern 1984; Filippenko 1985; Filippenko & Sargent 1988; Ho, Filippenko, & Sargent 1993). This conclusion has been corroborated by theoretical photoionization models (e.g., Ferland & Netzer 1983; Binette 1985). These studies strongly suggest that the basic mechanism that powers the activity is similar at all nuclear luminosities and scales with nuclear luminosity, a particularly appealing result because it allows a single unified model to explain the entire AGN phenomenon and eliminates models that cannot predict the observed properties simply by scaling with source luminosity.

Since AGN activity (as in quasars and Seyfert 1 galaxies) manifests itself over most of the electromagnetic spectrum, multiwavelength observations are important to determine if LLAGNs *are indeed* low-power versions of quasars. Many workers (Steiner 1981; Elvis, Soltan, & Keel 1984; Whittle 1992; Mulchaey et al. 1994) have found correlations between the emission-line properties and the continuum in various wavelength regimes. These correlations segregate the objects according to the luminosity of the central engine. Additionally, X-ray observations of quasars have enabled the construction of the X-ray luminosity function of powerful AGNs, critical to interpreting the X-ray background. Thus, our understanding of powerful AGNs, though not by any means complete, is quite advanced.

A careful analysis of LLAGNs with X-ray luminosities $L_X \approx 10^{41}$ ergs s^{-1} can be used to address the following questions. Is there an intrinsic lower limit to the luminosity of the AGN phenomenon? What fraction of galaxies contain compact massive objects that could give rise to nuclear activity? What is the shape of the X-ray luminosity function of AGNs at the low-luminosity end? How much do LLAGNs contribute to the X-ray background? Answers to these questions can improve our understanding of AGN evolution (e.g., Weedman 1985) and the cosmic X-ray background. Here we present the results of a study of five LLAGNs with the *ROSAT* High-Resolution Imager (HRI) and of three of these with the *ROSAT* Position Sensitive Proportional Counter (PSPC) to determine the distribution of X-rays in these objects and to see whether the dominant mechanism for the production of X-rays is the same at all AGN luminosities.

In § 2 we present the observations, and in § 3 we discuss the results of the analysis. Our conclusions are summarized in § 4.

2. OBSERVATIONS

Since we are interested in activity at low levels, we selected five LLAGNs with broad ($\geq$1000 km s^{-1}) Hα emission (Filippenko & Sargent 1985; Filippenko 1989) and line luminosities in the range 2×10^{39}–10^{40} ergs s^{-1}. Typical Hα emission-line luminosities for quasars and Seyfert 1 galaxies range between 10^{42} and 10^{45} ergs s^{-1}. If the soft X-ray and broad Hα luminosities in these LLAGNs have the same correlation as seen in quasars and Seyfert galaxies, we expect the X-ray luminosity to be $\sim 10^{41}$ ergs s^{-1}. Details of the LLAGNs and the observing times are given in Table 1. The galaxy types, redshifts (cz), magnitudes (B_T), and sizes are from the Third Reference Catalog of Bright Galaxies (de Vaucouleurs et al. 1991), and the Galactic column density ($N_{\rm HGal}$) is from Burstein & Heiles (1982). Throughout the analysis we use $H_0 = 50$ km s^{-1} Mpc^{-1} and $q_0 = 0$.

2.1. *ROSAT Observations*

The galaxies were observed with the *ROSAT* HRI for exposures ranging from 4000 s to 11,000 s (see Table 1). The HRI images were analyzed using the XRAY.XSPATIAL tool in IRAF. To determine the source counts, a region with radius 80 pixels (roughly 40″, or 4 times the full width at half-maximum [FWHM] of the HRI point-spread function [PSF]) centered on the source was used to determine the net counts, and an annulus around the source was used to determine the background counts. The net X-ray counts of each galaxy are given in Table 2. The signal-to-noise ratio (S/N) was given by S/N = net counts/(raw counts)$^{1/2}$. Subsequently, the count rates were converted into fluxes (see Table 2) by using the conversion factor 1 count s^{-1} = 1.96×10^{-10} ergs s^{-1} cm^{-2} (David et al. 1993). The conversion factor is based upon the number of counts in a 5×5 arcsec^2 cell which contains 50% of the total source counts. Hence, a factor of 2 correction had to be applied to the count rates determined by us to account for the large extraction region used. For the conversion we assumed a power-law X-ray spectral model with photon index 2.5 and $\log (N_{\rm H}/{\rm cm}^{-2}) = 20.7$. These model parameters are similar to the spectral parameters determined from the *ROSAT* PSPC data for the galaxies (see below). Contour maps of the HRI images are shown in Figure 1. It is seen from Figure 2 that the half-light diameter of the soft X-ray emission is $\sim$10″ (essentially unresolved), while Table 1 shows the optical diam-

TABLE 1

GENERAL PROPERTIES OF THE LOW-LUMINOSITY ACTIVE GALACTIC NUCLEUS SAMPLE

GALAXY NGC	TYPE	cz (km s^{-1})	B_T (mag)	D_{25}	$N_{\rm HGal}$ (10^{20} cm^{-2})	OBSERVING TIME HRI (ks)	PSPC (ks)	Optical (s)	OBSERVING DATE HRI	PSPC	Optical
3642.....	Sb	1588	11.65	5.37	1.43	9.98	8.8	1800	1992 Oct 25	1993 Oct 21	1986 Mar 28
4278.....	E1	649	11.09	4.07	1.75	9.55	3.4	900	1992 Dec 11	1993 Dec 16	1993 Apr 13
4639.....	Sb	1010	12.24	2.75	2.34	7.88	7.3	1800	1992 Dec 12	1993 Jun 30	1986 Mar 27
5033.....	SBc	878	10.75	10.71	1.06	4.33	...	1200	1992 Jun 25	...	1993 Jan 29
5273.....	S0/a	1054	12.44	2.95	0.93	10.77	...	900	1992 Jun 26	...	1993 Jun 28

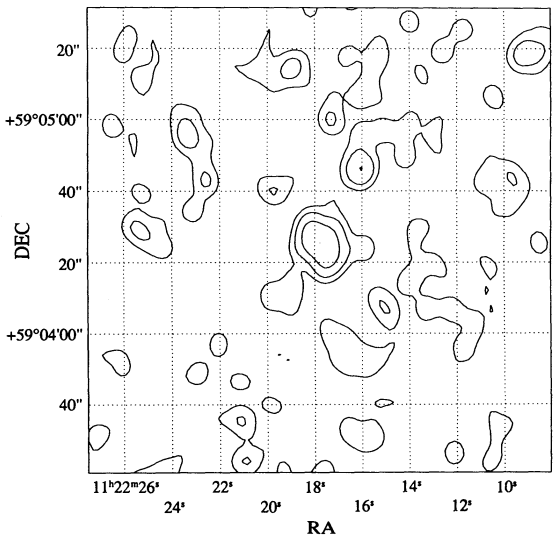

FIG. 1*a*

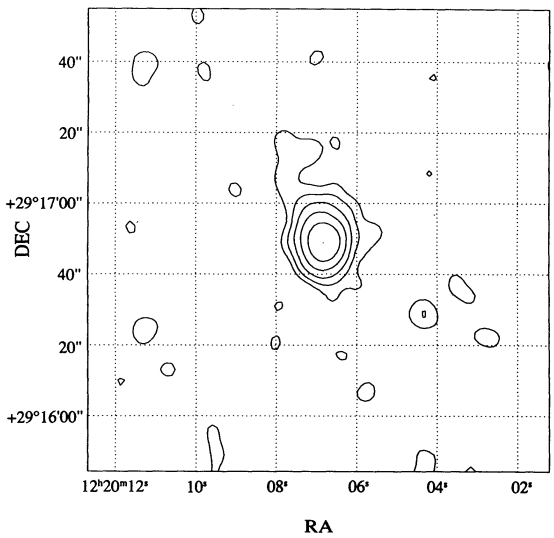

FIG. 1*b*

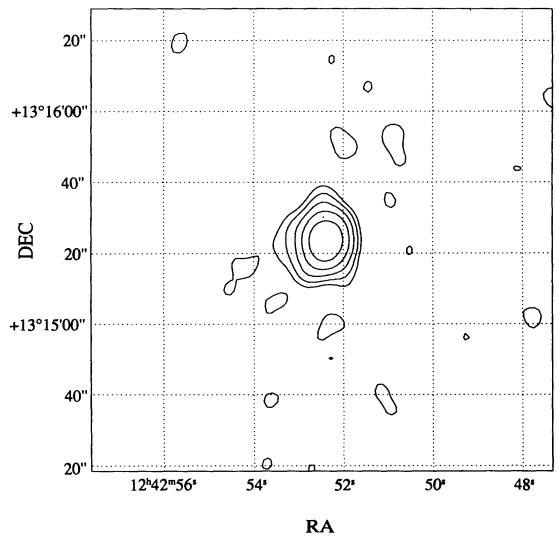

FIG. 1*c*

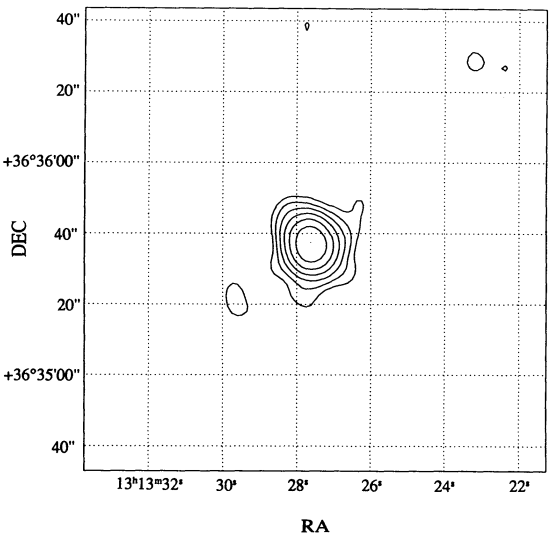

FIG. 1*d*

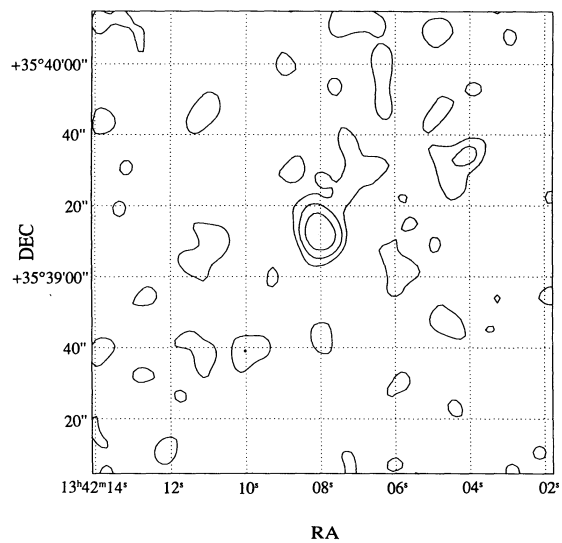

FIG. 1*e*

eter (D_{25}) of the galaxies to be 2.'8–10.'7. The HRI observations indicate that the soft X-rays are mostly nuclear.

To date we have acquired *ROSAT* PSPC data for three of the five galaxies in our sample: NGC 3642, NGC 4278, and NGC 4639. The data were corrected and rebinned using a technique similar to that of Turner, George, & Mushotzky (1993a). These data were analyzed using XSPEC, with different spectral models for the fits. The best fit was obtained by a model consisting of a power law including an absorption column. The fit parameters (mean photon index, Γ, total absorbing column, N_H, and the reduced chi squared, χ_r^2) and unabsorbed flux are given in Table 2. The spectra and the fits to the data are illustrated in Figure 3. The PSPC fluxes (0.2–2.2

FIG. 1.—Contour maps of the *ROSAT* HRI images in J2000 coordinates. Each pixel represents 1.''5. The contour levels are (*a*) NGC 3642: 0.37, 0.18, 0.09, and 0.05 counts pixel^{-1}; (b) NGC 4278: 2.50, 1.25, 0.63, 0.31, 0.16, and 0.08 counts pixel^{-1}; (*c*) NGC 4639: 2.24, 1.12, 0.56, 0.28, 0.14, and 0.07 counts pixel^{-1}; (*d*) NGC 5033: 5.28, 2.64, 1.32, 0.66, 0.33, 0.17, and 0.08 counts pixel^{-1}; and (*e*) NGC 5273: 0.47, 0.24, 0.12, and 0.06 counts pixel^{-1}.

TABLE 2

X-RAY DATA

Galaxy NGC	Net HRI Counts (counts)	HRI S/N	HRI Count Rate (counts s^{-1})	HRI Flux (10^{-12} ergs s^{-1} cm^{-2})	PSPC Flux (10^{-12} ergs s^{-1} cm^{-2})	Γ	N_H (10^{20} cm^{-2})	χ^2_ν
3642.....	33	3.5	0.0033	0.32	0.25	2.84 ± 0.67	4.1 ± 2.1	1.09
4278.....	182	11.9	0.0191	1.87	2.56	2.76 ± 1.15	5.4 ± 3.7	0.78
4639.....	161	11.4	0.0204	2.00	0.80	2.27 ± 0.40	3.9 ± 1.6	1.34
5033.....	311	16.9	0.0718	7.04	...	...	...	...
5273.....	33	3.4	0.0030	0.29	...	...	...	...

keV) are different from the HRI fluxes (0.2–2.2 keV) because we have used the canonical $\Gamma = 2.5$ and $\log (N_H/cm^{-2}) = 20.7$ to determine the HRI fluxes. We have not used the individual PSPC fit parameters to determine the HRI fluxes because the PSPC fit parameters are not well constrained, as shown in Table 2. The NGC 4639 spectrum exhibits residuals at ~ 1 keV, but the statistical significance of this feature is not high. The NGC 4278 spectrum has very low S/N due to the short exposure time, and hence the fit parameters are poorly constrained. The exposure time was prematurely terminated because of spacecraft problems at the time of the observation.

2.2. *Optical Observations*

Optical CCD spectra were obtained at Palomar Observatory for NGC 3642 and NGC 4639 and at Lick Observatory for NGC 5033, NGC 4278, and NGC 5273. The Palomar observations are described by Filippenko & Sargent (1985). The lick observations were taken with the Kast double spectrograph (Miller & Stone 1993), covering the approximate wavelength region 3200–9800 Å. The slit width was 2″. All the spectra were extracted with a window of 4″ along the slit, yielding an effective aperture of 8 arcsec^2. The data were reduced (flattened, sky subtracted, wavelength and flux calibrated) using standard methods (e.g., Filippenko & Sargent 1988). Atmospheric absorption lines were removed by division with stars having intrinsically featureless continua. Finally, the appropriate redshift was removed from each spectrum. These data were binned to 2 Å per pixel, and have, on average, a spectral resolution of 5 to 7 Å.

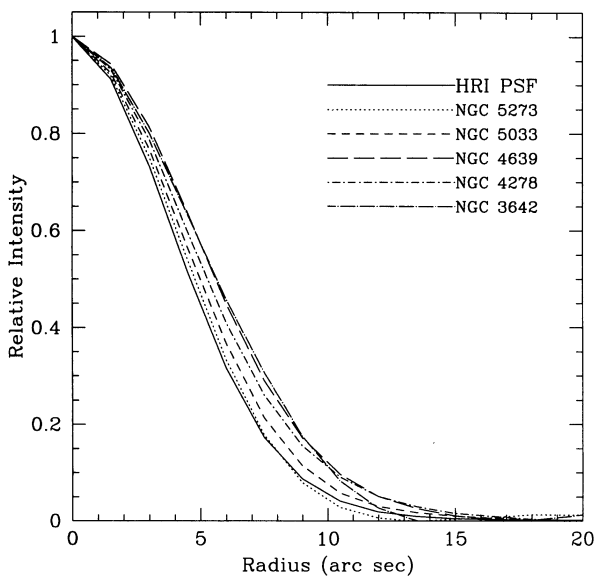

FIG. 2.—A comparison of the HRI point-spread function with the azimuthally averaged X-ray galaxy profile. This shows that the X-ray emission is entirely, or almost entirely, confined to the nucleus. The slight extension in four of the galaxies has low statistical significance.

Because the stellar component of the nuclear spectrum is significant in LLAGNs, it is important to correctly remove the stellar contribution in order to accurately measure the emission lines. Template galaxies observed under the same conditions, and closely matching the target galaxies in velocity dispersion and metallicity, were used to subtract the stellar contribution from each spectrum (see Ho et al. 1993).

The emission-line properties (FWHM and flux) were determined assuming Gaussian profiles. All the emission lines in the starlight-subtracted spectrum were fitted using the NGAUSSFIT routine in STSDAS. The general procedure used was as follows. The continuum and slope were set locally to a region ± 100 Å from the line center. In the first iteration all parameters of the narrow emission lines were allowed to vary. Subsequently, the centers of the narrow lines were fixed, and their FWHMs were set to that of [N II] λ6584; only the amplitude was allowed to vary. Of particular concern is the Hα + [N II] complex; the nitrogen and hydrogen lines are blended, and there is also a broad (>1000 km s^{-1}) component to the Hα emission. In this region, as well as that of Hβ, fits to the narrow-line components were made first. The FWHM and line center were fixed for these lines, but the narrow-line amplitude, and the broad line's FWHM, line center, and amplitude were allowed to vary. An additional constraint required that the [N II] $\lambda\lambda$6548 and 6584 lines maintain a 1:3 ratio in the flux. The fits obtained for the strong lines are good, with flux uncertainty of 10%. Weak lines, such as [O I] λ6300, have flux uncertainties as large as 40%.

The results of the fits are given in Table 3. The Gaussian fits to the Hα region for each galaxy are also shown in Figure 4. From the spectra one can see that the contribution of the broad component to the total Hα flux varies from 96% to 30% in the sample (see Table 4).

3. ANALYSIS AND DISCUSSION

3.1. *ROSAT HRI Images*

A comparison of the azimuthally averaged galaxy profiles with that of the HRI PSF (see Fig. 2) shows that the X-ray emitting gas is mostly nuclear. Although NGC 3642 appears to be extended when compared with the PSF, its HRI observation has only 33 counts in the nuclear region, and we cannot attribute any significance to the apparent extension.

The 5″ resolution of the *ROSAT* HRI corresponds to ~ 500 pc at the average distance of the galaxies in our sample; some of the X-ray emission could therefore be due to stars or supernovae. We have compared the (0.2–2.2 keV) X-ray luminosities of the galaxies in our sample with the predicted X-ray lumi-

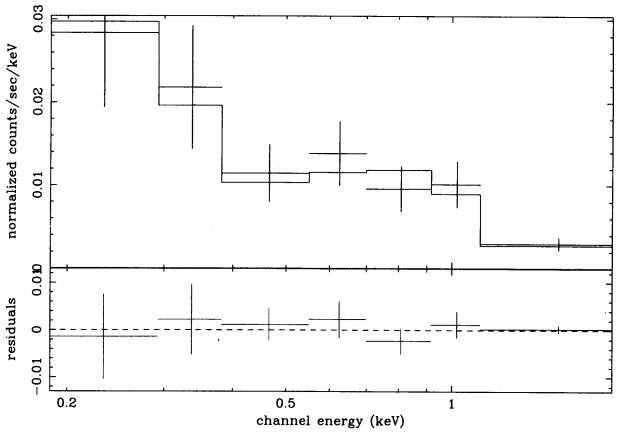

FIG. 3a

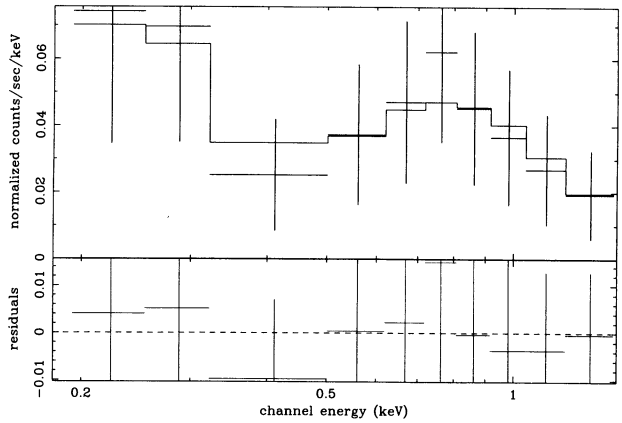

FIG. 3b

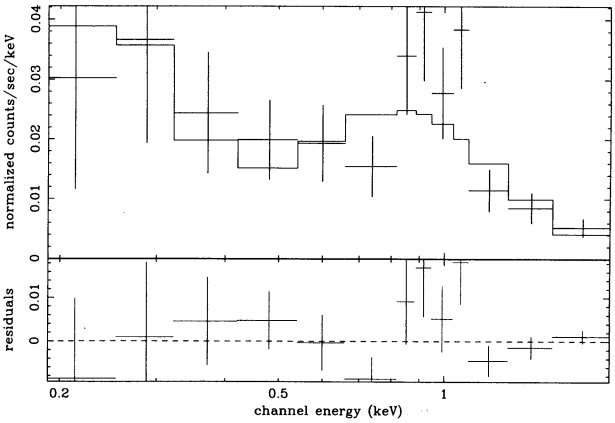

FIG. 3c

FIG. 3.—The power-law model fits to the *ROSAT* PSPC data: (*a*) NGC 3642, (*b*) NGC 4278, and (*c*) NGC 4639. The model fit parameters are given in Table 2.

nosities of normal disk and elliptical galaxies having the same absolute blue magnitude [log (L_X) predicted in Table 4], using the results in Fabbiano (1989). Our measured X-ray luminosities are 3–40 times greater than expected for normal galaxies, providing further evidence that the X-rays we observe are most likely due to an AGN or unusual nuclear source.

3.2. *Optical Spectra*

Since a broad Hα emission line (FWHM ≥ 1000 km s^{-1}, greater than the narrow forbidden lines) is present in all five galaxies of our sample, they are technically Seyfert 1 galaxies. However, if only the narrow-line intensity ratios are used, the galaxies can be classified as Seyfert galaxies or LINERs, based on the diagnostic line ratios (Baldwin, Phillips, & Terlevich 1981). The traditional dividing line between Seyfert galaxies and LINERs is at [O I] λ6300/[O III] λ5007 = 0.33 (Heckman 1980); thus NGC 3642 and NGC 4278 are LINERs, while NGC 4639, NGC 5033, and NGC 5273 are Seyfert galaxies. The intensity ratio of [O III] λ5007 to narrow Hβ supports these classifications; Seyfert galaxies generally have [O III] λ5007/Hβ > 3 (Osterbrock 1989). Interestingly, we also see a correlation with the prominence and width of the broad Hα

TABLE 3

OPTICAL EMISSION-LINE FLUXES

Line	NGC 3642[a] (10^{-15} ergs s^{-1} cm^{-2})	NGC 4278[b] (10^{-15} ergs s^{-1} cm^{-2})	NGC 4639[c] (10^{-15} ergs s^{-1} cm^{-2})	NGC 5033[d] (10^{-15} ergs s^{-1} cm^{-2})	NGC 5273[e] (10^{-15} ergs s^{-1} cm^{-2})
[O II] λ3727	17.01	215.30	...	27.40	37.70
Hβ narrow	5.86	45.02	0.93	13.42	16.79
Hβ broad	...	...	23.52	25.16	30.09
[O III] λ4959.....	1.38	16.91	1.87	13.14	35.78
[O III] λ5007.....	4.18	56.41	6.53	40.90	110.00
[O I] λ6300	1.70	39.06	1.82	8.33	8.44
[O I] λ6364	0.43	16.98	0.59	...	4.33
[N II] λ6548	3.05	43.64	1.83	32.87	13.30
[N II] λ6583	9.16	130.91	5.52	98.33	39.90
Hα narrow	16.13	114.60	5.08	56.50	49.60
Hα broad.....	12.63	49.50	117.80	170.40	242.20
[S II] λ6716	8.70	93.47	2.85	26.34	16.64
[S II] λ6731	5.95	77.31	2.89	15.78	17.00

[a] FWHM(narrow lines) ≈ 9 Å; FWHM(broad lines) ≈ 24 Å.
[b] FWHM(narrow lines) ≈ 12 Å; FWHM(broad lines) ≈ 63 Å.
[c] FWHM(narrow lines) ≈ 5 Å; FWHM(broad lines) ≈ 78 Å; spectrum does not extend down to λ3727.
[d] FWHM(narrow lines) ≈ 9 Å; FWHM(broad lines) ≈ 70 Å.
[e] FWHM(narrow lines) ≈ 7 Å; FWHM(broad lines) ≈ 60 Å.

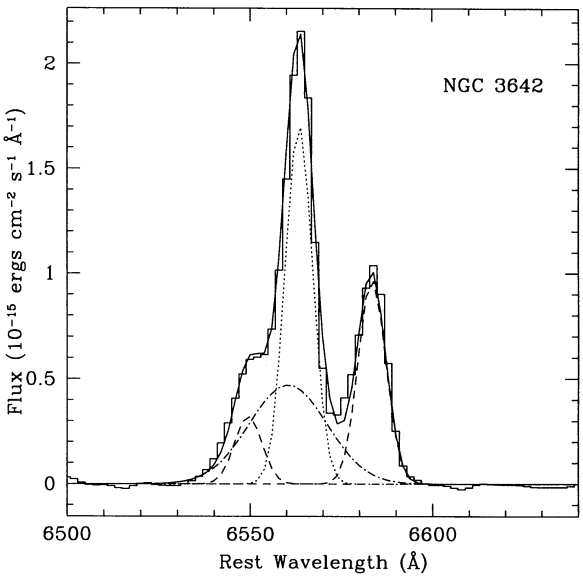

FIG. 4*a*

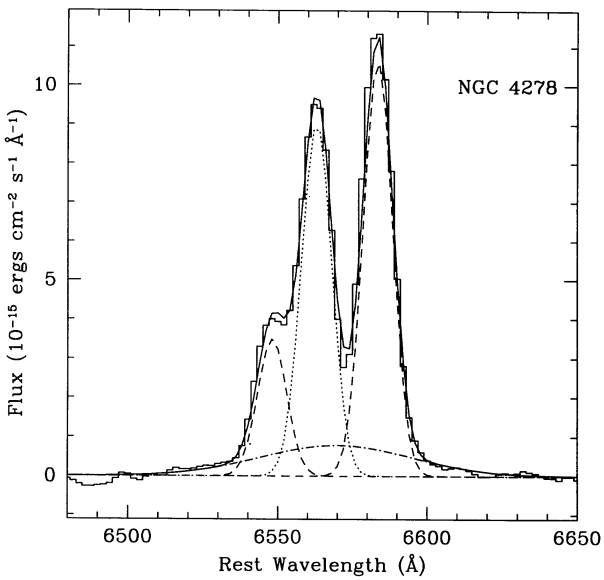

FIG. 4*b*

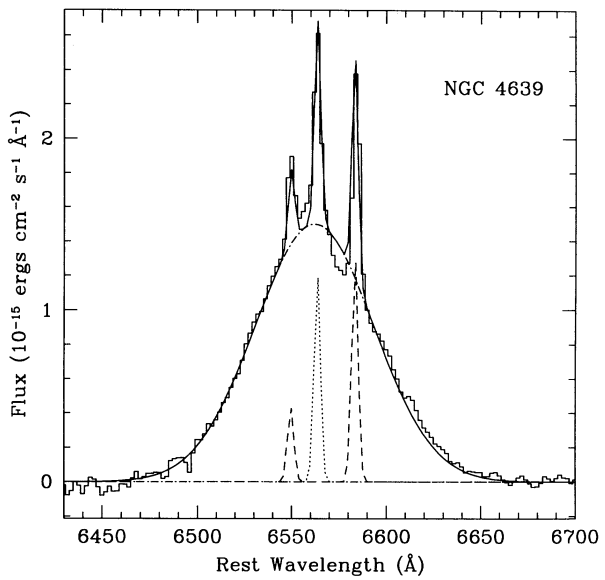

FIG. 4*c*

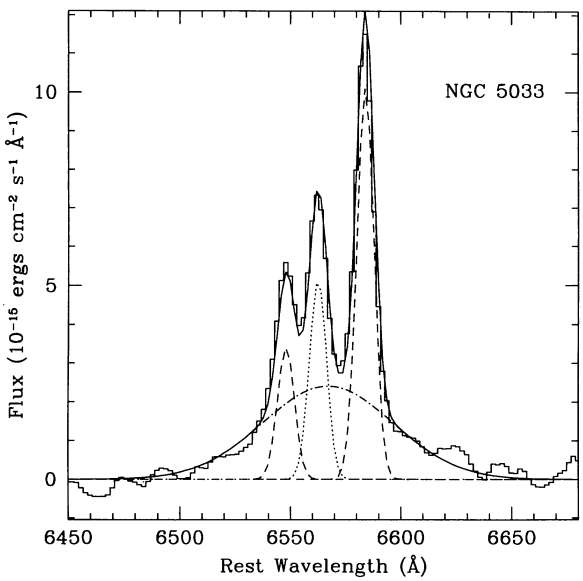

FIG. 4*d*

FIG. 4.—The Gaussian fits to the Hα + [N II] region. The data are shown as a histogram, and the fit as a smooth line. Individual components include [N II] (*dashed line*), narrow Hα (*dotted line*), and broad Hα (*dot-dashed line*). Wavelengths are given in the rest frame of each galaxy.

TABLE 4

X-RAY AND OPTICAL LUMINOSITIES

Galaxy NGC	log (L_X) (0.2–2.2 keV) (ergs s^{-1})	log (L_X) Predicted (ergs s^{-1})	log ($L_{H\alpha}$) Total (ergs s^{-1})	Ratio of Broad Hα to Total Hα	log (νP_ν) at 2500 Å (ergs s^{-1})	α_{ox}
3642.....	40.59	40.1	39.54	0.44	41.66	1.74
4278.....	40.58	39.5	39.51	0.30	41.00	1.49
4639.....	40.99	39.4	39.78	0.96	...	...
5033.....	41.41	39.9	39.91	0.75	41.44	1.33
5273.....	40.19	39.3	40.19	0.83	41.30	1.75

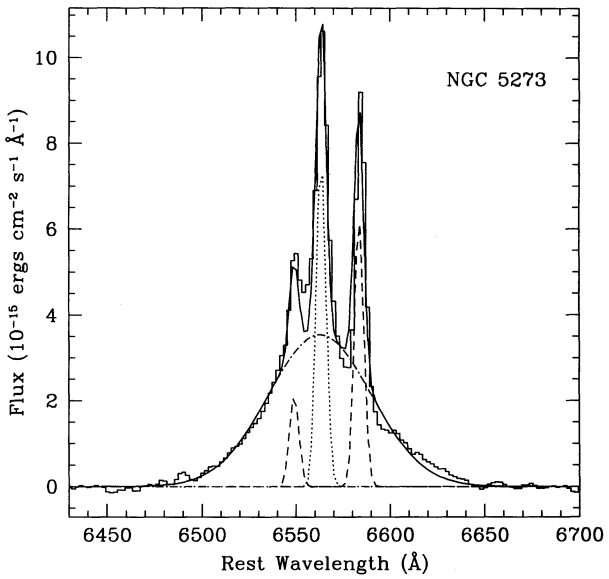

FIG. 4e

emission (Table 4). The Seyfert galaxies have very wide ($\gtrsim$2700 km s^{-1}) and strong broad components in their Hα line profiles, while the LINERs have narrower ($\lesssim$2200 km s^{-1}) and weaker (relative to the narrow component) broad components.

3.3. *ROSAT PSPC Data*

For the PSPC data of NGC 3642 and NGC 4639, a power law provides a much better fit than either a blackbody or a Raymond-Smith thermal plasma (Raymond & Smith 1977; see Fig. 3 and details of the fit in Table 2). Our sparse PSPC data indicate that the mean photon index (Γ) of LLAGNs (2.6) is similar to that of other Seyfert galaxies (Turner et al. 1993a; Mulchaey et al. 1993). Seyfert 1 galaxies have a mean Γ of 2.38 $\pm$ 0.25 in the 0.2–2.2 keV *ROSAT* band, steeper than the canonical Γ of 1.7 observed in the 2–10 keV band.

The Seyfert galaxies Mrk 3, NGC 1365 (Turner, Urry, & Mushotzky 1993b) and the LINER NGC 2639 (Reichert, Mushotzky, & Filippenko 1994) show an emission-line complex with a large equivalent width at $\sim$1 keV in their PSPC spectra. Turner et al. (1993b) postulate that this line complex could be due to iron L and ionized oxygen. We find that NGC 4639 also exhibits residuals at approximately 1 keV, albeit at low statistical significance. The LLAGNs in our sample, along with those in Reichert et al. (1994), show evidence for a complex spectrum.

For our sample we find the total absorbing columns to be approximately (4–5) $\times$ 10^{20} cm^{-2} (Table 2). Reichert et al. (1994) and Petre et al. (1993) derive similar total absorbing columns for the LLAGNs in their samples. This observational evidence is contrary to the suggestion of Lawrence & Elvis (1982) that soft X-rays in LLAGNs are highly absorbed. Comparison of Tables 1 and 2 shows that the total derived absorbing column density is approximately 2–3 times the Galactic absorbing column. Hence, these LLAGNs do not have their thick intrinsic absorbing columns ($\gtrsim 10^{22}$ cm^{-2}) observed in some AGNs with higher luminosities.

3.4. *X-Rays versus* Hα

Kriss, Canizares, & Ricker (1980) showed that a strong correlation exists between the soft X-ray luminosity and the broad Hβ (and therefore broad Hα) line luminosity in quasars and Seyfert 1 galaxies (see also Steiner 1981). If the dominant mechanism for the production of X-rays is the same, then we would expect any correlation seen at the high-luminosity range to continue down into the low-luminosity range. This is indeed the case, as shown in Figure 5.

In order to compare our LLAGNs to the more luminous AGNs, we searched through the literature for Seyfert galaxies and quasars with published soft X-ray and emission-line luminosities. The data were obtained primarily from Whittle (1992), De Robertis & Dahari (1988), and Steiner (1981), which contain the most complete line and X-ray luminosities for a large number of AGNs. In these papers the X-ray luminosities for the Seyfert galaxies and quasars are *Einstein Observatory* IPC values; the emission-line data are heterogeneous and originate from either the authors' own observations or are taken by them from the published literature. Since the energy band and the detector response of the *ROSAT* HRI and the *Einstein Observatory* IPC are similar, we can compare the X-ray fluxes from these references with those of our sample of LLAGNs. The X-ray luminosities given by Steiner (1981) refer to the 0.5–4.5 keV band, while those in De Robertis & Dahari (1988) refer to the 0.2–4.0 keV band. To compare the various data sets and remove known systematic effects on average, we have multiplied the Steiner data by 2.7, and the De Robertis & Dahari data by 1.4. These factors were derived for a power-law model with photon index 2.5; despite being model dependent, they provide a reasonable first-order correction to the X-ray luminosities obtained in different bandpasses.

The correlation between the soft X-ray luminosity and the Hα emission-line luminosity for quasars and Seyfert galaxies is shown in Figure 5, while Figure 6 illustrates the correlation

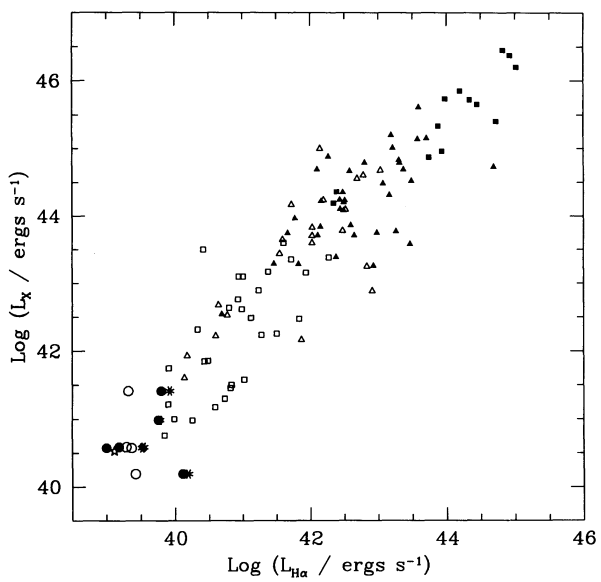

FIG. 5.—The correlation between the luminosity in the X-ray band with the luminosity in the Hα emission line. The quasars (*filled squares*) and Seyfert 1 galaxies (*filled triangles*) are from Steiner (1981). Seyfert 1 galaxies (*open triangles*) and Seyfert 2 galaxies (*open squares*) are from Whittle (1992) and De Robertis & Dahari (1988). The Seyfert 1 galaxies (*open triangles*) in Whittle's data did not have Hα fluxes but did have Hβ fluxes; for these objects the Hβ flux was multiplied by 3 to get the Hα flux. For the LLAGNs in our sample, the total Hα flux is represented by asterisks, the narrow Hα flux by open circles, and the broad Hα flux by filled circles. M81 is represented by a star.

using fluxes. On the same figures we have plotted each of the LLAGNs in our sample 3 times: once each using their broad, narrow, and total Hα flux so as to closely match the Seyfert galaxies and quasars in terms of comparing nuclear activity. The Balmer lines of quasars and Seyfert 1 galaxies are dominated by the broad component, while at the other extreme, the Balmer lines of Seyfert 2 galaxies are dominated by the narrow component. Therefore, in order not to a priori bias our conclusions regarding the nature of the LLAGNs, we plot our sample as discussed above. The X-ray luminosity from Boller et al. (1992) and the Hα luminosity from Filippenko & Sargent (1988) for M81 are also shown in Figures 5 and 6. The Spearman-rank test applied to the data in Figure 5 (using the total Hα luminosity for the LLAGNs) gives a correlation coefficient of 0.88, with a probability of 99.99% that the data are correlated. We find that the correlation between the luminosity in the X-ray band and the luminosity in the Hα emission line does indeed extend to the low-luminosity objects. From Figure 6 we see that the L_X versus $L_{H\alpha}$ correlation is not dominated by the distance effect, since there is also a correlation in the fluxes (Spearman-rank correlation coefficient 0.93, with a probability of 99.99%, using the total Hα flux for the LLAGNs). Figure 5 encompasses over six orders of magnitude in luminosity, and we see that the correlation appears to extend to the low-luminosity objects, suggesting that these galaxies contain true active nuclei. The mean $L_X/L_{H\alpha}$ ratio of the LLAGNs is ~ 14, with a range of 1–32 for the individual $L_X/L_{H\alpha}$ ratios. For comparison, the mean $L_X/L_{H\alpha}$ ratio for AGNs is ~ 29, with a range of 1–100.

If the emission mechanism in the luminous AGNs and the LLAGNs is exactly the same, we expect the correlations in Figures 5 and 6 to be tight. There are several ways of introducing scatter in the figures. One is the lack of homogeneity in the compiled data. But perhaps the more important source of scatter is variability. If LLAGNs are as variable as more luminous AGNs, individual observations at very different epochs will shown large scatter. Seyfert galaxies are known to vary up to a factor of 2 in their Hα flux (Robinson 1994), while their X-ray fluxes show even larger variations. Thus, the scatter in Figures 5 and 6 could largely be due to variability of the objects.

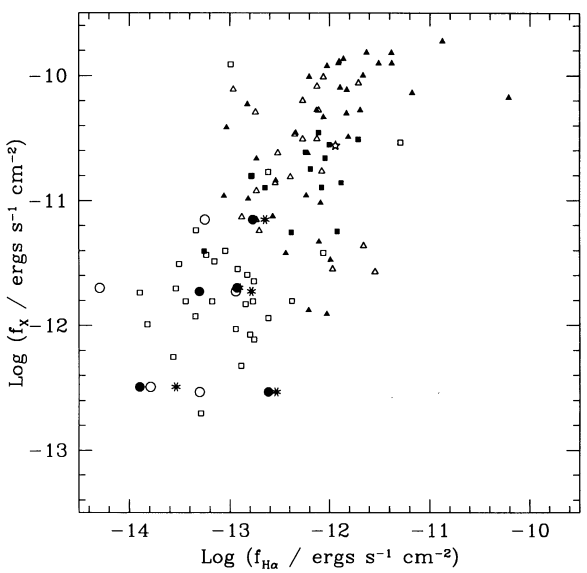

FIG. 6.—The correlation between the flux in the X-ray band with the flux in the Hα emission line. The symbols are the same as in Fig. 5.

For the objects in our sample, there is no evidence of a nonstellar ionizing continuum in the optical. All the LLAGNs except NGC 4639 have been observed in the UV by the *International Ultraviolet Explorer* (*IUE*), and they are extremely faint in the UV. Following Mushotzky & Wandel (1989), the "optical" (actually UV) to X-ray spectral index (α_{OX}) was defined between $\nu_O = \nu(2500\ \text{Å})$ and $\nu_X = \nu(2\ \text{keV})$ as follows:

$$\alpha_{OX} = -\frac{\log (F_O/F_X)}{\log (\nu_O/\nu_X)} ,$$

where F_O and F_X are the fluxes at 2500 Å and 2 keV, respectively. The value of F_X was determined from the 0.1–2.4 keV broadband flux (P_X) assuming a photon index of 2.5:

$$\log F_X = \log P_X - 18.54 .$$

The values for α_{OX} and monochromatic luminosity at 2500 Å (νP_ν) are given in Table 4. Note that the former are actually *upper limits* because we have assumed that all the UV flux observed in the large aperture of *IUE* is due to the AGN, which may not be the case. Images in the UV continuum with the *Hubble Space Telescope* will be required to determine the UV flux associated with the compact nuclear source in each galaxy.

Our average value of α_{OX} is 1.6 (an upper limit, as explained above). For comparison, the average value of α_{OX} determined by Mushotzky & Wandel (1989) for luminous type 1 Seyfert galaxies is 1.36. They have calculated the flux density at 2 keV from different data (*Einstein Observatory*, 0.5–4.5 keV) and with a different model (power law, $\Gamma = 1.5$) than we have used. Newer *ROSAT* data on Seyfert galaxies (Turner et al. 1993a) suggest that a more appropriate model choice would be a double–power-law model with $\Gamma = 2.5$ from 0.5 to 2.0 keV, and $\Gamma = 1.7$ (the canonical value for the harder X-ray photon index) from 2.0 to 4.5 keV. Using this model, the Mushotzky & Wandel values for α_{OX} would be increased by about 0.06, to an average of 1.42. This correction is quite small compared with the scatter in α_{OX} within their sample or ours. Thus, our newly determined values for α_{OX} are consistent with the values for considerably more powerful AGNs.

Reichert et al. (1994) have used *ROSAT* to study a small sample of LINERs, and Petre et al. (1993) have likewise studied the prototypical LLAGN M81 using BBXRT. Both groups find evidence that these galactic nuclei have smaller values of α_{OX} than our sample (α_{OX} about 1.0). However, keeping in mind that our values of α_{OX} must be treated as upper limits (see above), our results are probably also consistent with theirs.

4. CONCLUSIONS

1. Our *ROSAT* HRI images of five LLAGNs show that their X-ray emission is mostly or entirely confined to the nucleus ($r \lesssim 500$ pc).

2. Our sparse PSPC data indicate that the LLAGNs can be fitted with a power law whose photon index (2.6) is similar to that of the more luminous AGNs (2.4) in the *ROSAT* band (0.2–2.2 keV). NGC 4639 shows a possible feature at 1 keV which may be due to the Fe L complex. In addition, the LLAGNs have a low intrinsic absorption column ($\sim$[4–5] $\times 10^{20}$ cm^{-2}) compared to more luminous AGNs.

3. We find that the correlation between X-ray and Hα luminosity seen in quasars and classical Seyfert 1 galaxies extends to low-luminosity objects. The mean $L_X/L_{H\alpha}$ ratio of LLAGNs is about 14, comparable to that of AGNs (about 29; both values have a large dispersion). This suggests that LLAGNs could be physically similar to luminous AGNs.

4. Using four of our LLAGNs, we derive an average upper limit of 1.6 for α_{OX}, consistent with the measured values for luminous AGNs (1.4, on average) and the prototypical LLAGN M81 (1.0).

To summarize, we find that while LLAGNs do follow the general trends seen in more luminous AGNs, the present data do not allow us to firmly conclude that the detailed X-ray emission mechanism in LLAGNs is the same as in the more luminous objects. Better data on the multiwaveband nonstellar continuum in a larger sample of LLAGNs is needed to assess the relationship between LLAGNs and their more powerful counterparts.

A. K. would like to thank the *ROSAT* staff at NASA/GSFC for their untiring help in reducing the *ROSAT* data. This project was funded by NASA grant NAG 5-2153. A. V. F. acknowledges the support of NSF grant AST 89-57063. We thank Tom Matheson for assisting with the Lick observations. This research has made use of the NASA/IPAC Extragalactic Database (NED), which is operated by the Jet Propulsion Laboratory, California Institute of Technology, under contract with the National Aeronautics and Space Administration.

REFERENCES

Baldwin, J. A., Phillips, M. M., & Terlevich, R. 1981, PASP, 93, 5
Binette, L. 1985, A&A, 143, 334
Boller, T., Meurs, E. J. A., Brinkman, W., Fink, H., Zimmermann, U., & Adrof, H.-M. 1992, A&A, 261, 57
Boyle, B. J., Griffiths, R. E., Shanks, T., Stewart, G. C., & Georgantopoulos, I. 1993, MNRAS, 260, 49
Boyle, B. J., Jones, L. R., & Shanks, T. 1991, MNRAS, 251, 482
Burstein, D., & Heiles, C. 1982, AJ, 87, 1165
David, L. P., Harnden, F. R., Jr., Kearns, K. E., & Zombeck, M. V. 1993, The *ROSAT* High Resolution Imager (Cambridge: Harvard-Smithsonian Center for Astrophysics)
De Robertis, M., & Dahari, O. 1988, ApJS, 67, 249
de Vaucouleurs, G., et al. 1991, The Third Reference Catalog of Bright Galaxies (New York: Springer-Verlag)
Elvis, M., Soltan, A., & Keel, W. 1984, ApJ, 283, 479
Fabbiano, G. 1989, ARA&A, 27, 87
Ferland, G. J., & Netzer, H. 1983, ApJ, 264, 105
Filippenko, A. V. 1985, ApJ, 289, 475
———. 1989, in Active Galactic Nuclei, ed. D. E. Osterbrock & J. S. Miller (Dordrecht: Kluwer), 495
———. 1994, in The Nearest Active Galaxies, ed. J. E. Beckman, L. Colina, & H. Netzer (Madrid: CSIC), 259
Filippenko, A. V., & Halpern, J. P. 1984, ApJ, 285, 458
Filippenko, A. V., Ho., L. C., & Sargent, W. L. W. 1993, ApJ, 410, L75
Filippenko, A. V., & Sargent, W. L. W. 1985, ApJS, 57, 503
———. 1986, in Structure and Evolution of Active Galactic Nuclei, ed. G. Giuricin et al. (Dordrecht: Reidel), 21
———. 1988, ApJ, 324, 134
———. 1989, ApJ, 342, L11
Halpern, J., & Steiner, J. E. 1983, ApJ, 269, L37
Heckman, T. 1980, A&A, 87, 152
———. 1987, in Observational Evidence of Activity in Galaxies, ed. E. Ye. Khachikian, K. J. Fricke, & J. Melnick (Dordrecht: Reidel), 421
Ho, L. C., Filippenko, A. V., & Sargent, W. L. W. 1993, ApJ, 417, 63
Keel, W. 1983a, ApJ, 269, 466
———. 1983b, ApJS, 52, 229
Kriss, G. A., Canizares, C. R., & Ricker, G. R. 1980, ApJ, 242, 492
Lawrence, A., & Elvis, M. 1982, ApJ, 256, 410
Miller, J. S., & Stone, R. P. S. 1993, Lick Obs. Tech. Rep., No. 66
Mulchaey, J. S., et al. 1993, ApJ, 414, 144
Mulchaey, J. S., Koratkar, A. P., Ward, M. J., Wilson, A. S., Whittle, M., Antonucci, R. R. J., Kinney, A. L., & Hurt, T. 1994, ApJ, 436, 586
Mushotzky, R. F., & Wandel, A. 1989, ApJ, 339, 674
Osterbrock, D. E. 1989, Astrophysics of Gaseous Nebulae and Active Galactic Nuclei (Mill Valley, CA: University Science)
Peimbert, M., & Torres-Peimbert, S. 1981, ApJ, 245, 845
Petre, R., Mushotzky, R. F., Serlemitsos, P. J., Jahoda, K., & Marshall, F. E. 1993, ApJ, 418, 644
Phillips, M. M., Charles, P. A., & Baldwin, J. A. 1983, ApJ, 266, 485
Phillips, M. M., Jenkins, C. R., Dopita, M. A., Sadler, E. M., & Binette, L. 1986, AJ, 92, 1062
Raymond, J. C., & Smith, B. W. 1977, ApJS, 35, 419
Reichert, G. A., Mushotzky, R. F., & Filippenko, A. V. 1994, in The First *ROSAT* Science Symp., ed. E. M. Schlegel & R. Petre (New York: AIP), in press
Robinson, A. 1994, in Reverberation Mapping of the Broad-Line Region in Active Galactic Nuclei, ed. P. M. Gondhalekar, K. Horne, & B. M. Peterson (San Francisco: ASP Conf. Ser., 69), in press
Rose, J. A., & Cecil, G. 1983, ApJ, 266, 531
Rose, J. A., & Searle, L. 1982, ApJ, 253, 556
Shuder, J. M. 1981, ApJ, 244, 12
Stauffer, J. R. 1983a, ApJ, 262, 266
———. 1982b, ApJS, 50, 517
Steiner, J. E. 1981, ApJ, 250, 469
Terlevich, R., Melnick, J., & Moles, M. 1987, in Observational Evidence of Activity in Galaxies, ed. E. Ye. Khachikian, K. J. Fricke, & J. Melnick (Dordrecht: Reidel), 499
Terlevich, R., Tenorio-Tagle, G., Franco, J., & Melnick, J. 1992, MNRAS, 255, 713
Turner, J., George, I. M., & Mushotzky, R. F. 1993a, ApJ, 412, 72
Turner, J., Urry, M., & Mushotzky, R. F. 1993b, ApJ, 418, 653
Weedman, D. W. 1985, in Astrophysics of Active Galaxies and Quasi-Stellar Objects, ed. J. S. Miller (Mill Valley, CA: University Science), 497
Whittle, M. 1992, ApJS, 79, 49
Yee, H. K. C. 1980, ApJ, 241, 894